Attenuation and Source Characteristics of the June 23, 2010 M5.0 Val-des-Bois, Quebec earthquake

Gail M. Atkinson and Karen Assatourians
Dept. Earth Sciences, University of Western Ontario
Submitted to Seism. Res. L.., June 29, 2010: Accepted July 13, 2010

Abstract

The **M**5.0 June 23, 2010 Val-des-Bois, Quebec earthquake produced a rich instrumental and felt ground- motion database. We use instrument-corrected response spectra and Fourier amplitude data from 120 stations, at distances from 60 to 1000 km, to examine the attenuation and source characteristics of this important event. The Val-des-Bois earthquake produced relatively-large response spectral amplitudes at distances less than 200 km, greater than predicted by most recent ground-motion prediction equations (GMPEs) (including the Atkinson and Boore, 2006 equations). By contrast, reported intensities at regional distances tended to be smaller than predicted by intensity GMPEs (Atkinson and Wald, 2007), although they were high in the epicentral area. From recent moderate earthquakes in eastern North America (ENA) (2010 Val-des-Bois and the 2005 Riviere du Loup event), we have learned that amplitudes at near distances are not well-predicted by average attenuation shapes drawn to pass through regional observations. To infer the source spectrum or near-source motions, we suggest the use of seismic moment as a constraint on the level of the source spectrum. Using Q-corrected observations to deduce the source-spectral shape, and the known seismic moment to fix its absolute amplitude level, we obtain an apparent source spectrum for the Val-des-Bois earthquake. The Val-des-Bois source spectrum is well described by a Brune model with a stress drop of 250 bars. Future work will focus on resolving near-source attenuation issues to provide better GMPEs for ENA over all magnitudes.

Introduction

The moment magnitude **M** 5.0 Val-des-Bois, Quebec earthquake of June 23, 2010 (45.904, -75.497) was a northwest-striking thrust event located approximately 60 km north of Ottawa, at a depth of 22 km (R. Herrmann; see Data and Resources). It was felt over an area of approximately 3 million km^2, throughout Quebec, Ontario, and U.S. states from Maine to Illinois to Kentucky, producing the strongest shaking ever felt in Canada's capital city, and the largest-ever on-line DYFI (Did You Feel It?) response (>57,000 responses). The Val-des-Bois earthquake was the largest event to shake southeastern Canada and the northeastern U.S. since the 2002 **M**5.0 Au Sable Forks, N.Y. earthquake. With an epicentral intensity of VII, it caused minor damage to several structures in the epicentral area, including reports of a badly-damaged church steeple, and cracked and fallen masonry (CBC News, June 23, 2010); windows were broken 60 km away in the Ottawa City Hall, and many buildings were evacuated (including the Parliament Buildings). There was also some road and bridge damage in the epicentral area, which was the result of embankment failure (Tinawi, pers. comm.., 2010).

The Val-des-Bois earthquake has provided a rich dataset for analysis, with 120 instrumental recording stations within 1000 km (with 9 3-component records at <100 km), in addition to the felt data. Figure 1 shows the locations of strong-motion and seismographic stations that recorded the earthquake, along with contours that provide a snapshot of the recorded motions. The contours are drawn by interpolating the inferred Modified Mercalli Intensity (MMI) across the region, as calculated from the recorded peak ground velocity (PGV) using the relationship between MMI and PGV from Atkinson and Kaka (2007); this is the same concept as employed in ShakeMap (Wald et al., 1999).

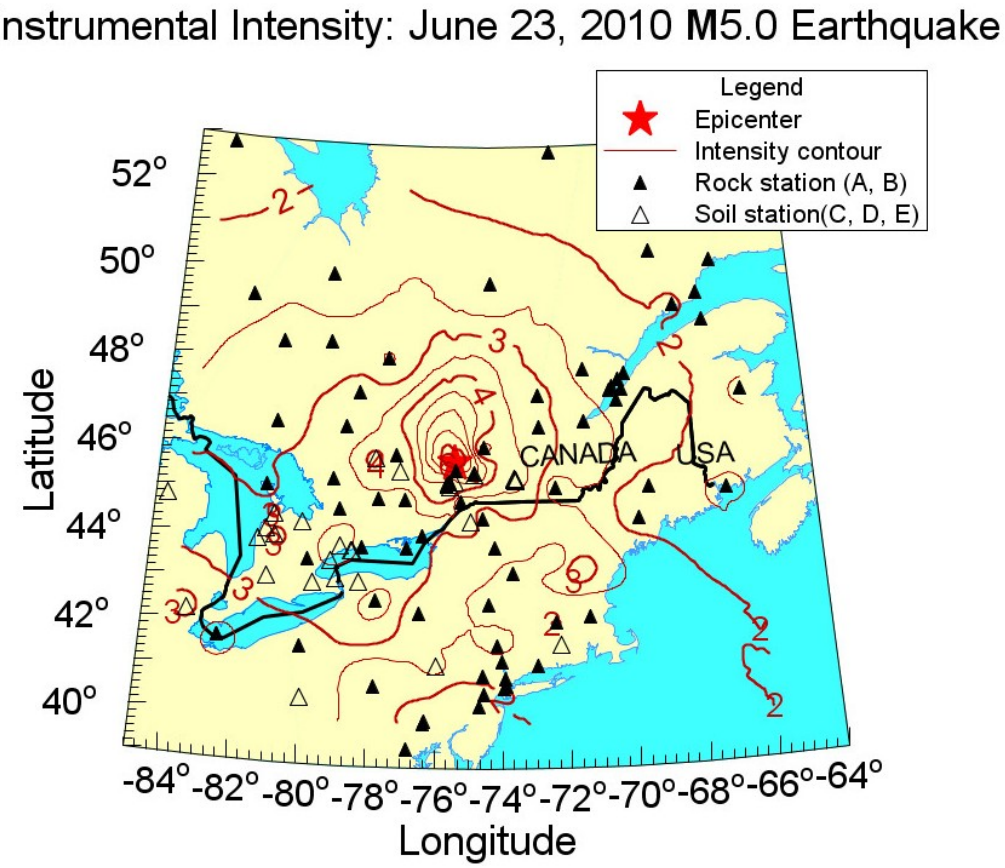

Figure 1 *– Overview of ground motions from the 2010* ***M****5.0 Val-des-Bois earthquake. Symbols show locations of recording stations. Contours show MMI as calculated from the recorded PGV values, using the relationship of Atkinson and Kaka (2007).*

In this note, we present processed ground-motion data from this important earthquake. We use the data to characterize the attenuation and apparent source spectrum in comparison to other similar-sized events in the region; we also examine the relationship between the recorded ground motions and felt effects. The work is particularly timely in light of the "Next Generation Attenuation – East" (NGA-East) community initiative that is currently underway to develop new ground-motion prediction equations (GMPEs) for eastern North America (ENA).

Instrumental Ground Motion Data in Comparison to GMPEs

Figure 1 summarizes the locations of recorded ground motions and their intensity. Table 1 provides the details of station locations, site conditions, and comments on signal characteristics for each record. For sites where no information on site condition was available, we assumed a site condition of "rock" or "soil" based on spectral shape, by comparing to other stations at similar distances with known site conditions. There are processed records from 120 stations, mostly 3-component broadband on rock, at epicentral distances from 48 to 1160 km. Two broadband seismographic records at R<100 km clipped (GAC and OTT), and were excluded from Table 1 and further analyses. The records were processed to produce instrument-corrected time series and calculate Fourier acceleration spectra (FA) and 5% damped pseudo-acceleration (PSA). The processing procedures are as described by Assatourians and Atkinson (2008; 2010) (see Data and Resources section). To summarize, a time window of 600s duration from the signal onset is selected for processing. A 2% taper is applied to the window. First-order Butterworth bandpass filters with low-cut and high-cut values of 0.1 Hz and 50 Hz, respectively, are applied. Instrument response is removed from the data in the frequency domain, and corrected acceleration time series are obtained. The frequency range from 0.1Hz to 50Hz is divided into 200 logarithmically-equal intervals; PSA and FA (log-averaged over the frequency interval) are calculated at these frequencies for all corrected signals. The data processing procedures have been checked by comparison against a number of standard programs, as described by Assatourians and Atkinson (2008).

Figure 2 plots the PSA values versus distance at two selected frequencies, in comparison to several ENA GMPEs; the plotted relations are those of Atkinson and Boore (2005) (stochastic model relations, as used in the 2010 National Building Code of Canada), Campbell (2003) (hybrid empirical relations), Atkinson and Boore (2006) (which replaced AB05), and Atkinson (2008) (based on a referenced empirical method). All the GMPEs are plotted for hard-rock sites, whereas the observations include both rock and soil sites. (Note: an approximate conversion of the Atkinson, 2008 relations from B/C to hard rock was made, using factors deduced from Atkinson and Boore, 2006.) The amplifications on soil sites in parts of southeastern Canada and the northeastern U.S. can be very large, due to the prevalence of soft marine sediment deposits overlying hard glacially-scoured rock, setting up ideal conditions for strong amplification and resonant effects (Motazedian and Hunter, 2008). As noted in Table 1, examination of the Fourier spectra of soil recordings in the region suggest that peak amplification factors of 5 to 10 are not uncommon. Such amplification factors are not properly handled by the "standard" soil amplification factors in typical GMPEs (eg. Boore and Atkinson, 2008 and other "NGA" site factors). The amplification factors in typical GMPEs describe broadband amplifications that result from moderate velocity gradient effects in typical western profiles; these factors would not accommodate the amplification peaks that result from resonance or very pronounced site effects. Thus in viewing the level of the recorded PSA values in comparison to the GMPEs, only the rock recordings should really be considered.

It is clear from the rock recordings that all of the GMPEs under-predict the PSA observations at <200 km by a large factor; this is especially so for the observations in the 50 to 70 km distance range. The under-prediction is most pronounced for the Atkinson

and Boore (2006) relations. This is disturbing, as the motions from the 2005 **M**4.7 Riviere du Loup, Quebec earthquake were also significantly under-predicted by AB06 in this distance range, at high frequencies. Recent work by Atkinson and Morrison (2009) and Atkinson et al. (2010), based on comparisons of earthquake motions in ENA versus California, have suggested that the AB06 GMPEs likely underpredict **M**5 motions at <100 km, while slightly overpredicting **M**6 to **M**7 motions at close distances. These observations tend to support that inference (at least for **M**5), as will be discussed in more detail later.

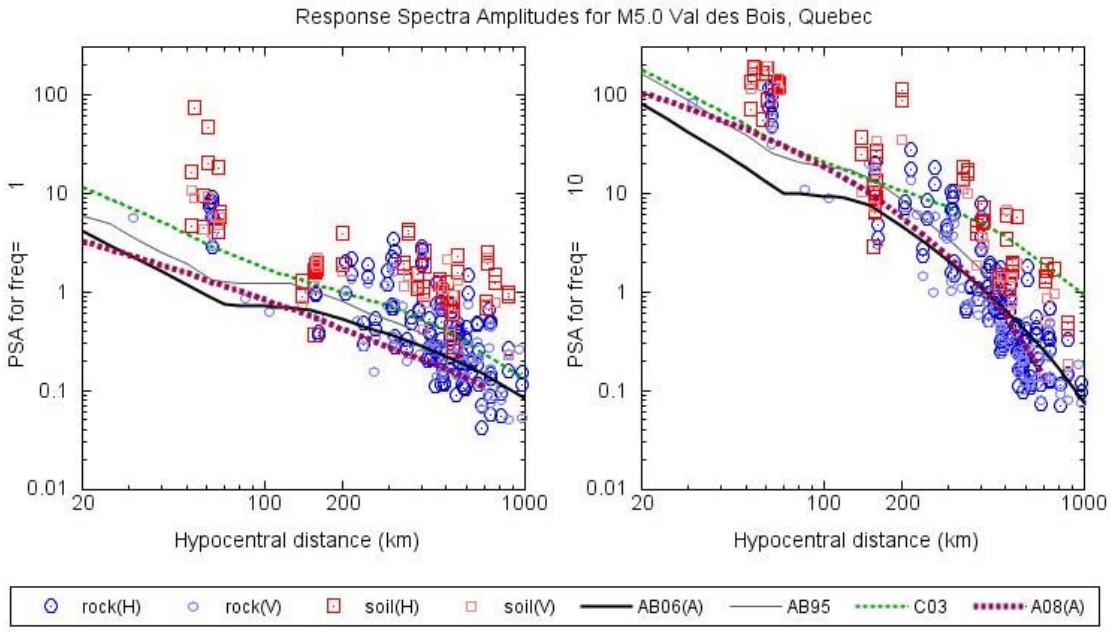

Figure 2 *– PSA observations (1 Hz, 10 Hz, in cm/s^2) from the Val-des-Bois earthquake, in comparison to selected ENA GMPEs for hard rock sites (Atkinson and Boore (2006; 1995); Atkinson, 2008; Campbell, 2003). Blue symbols are rock sites, red symbols are soil sites. Smaller symbol size denotes vertical component.*

The attenuation curve in the stochastic-model GMPE of AB06 has a hinged trilinear decay shape, as did the earlier AB95 version; Campbell (2003) also adopted the trilinear shape (AB95 version) for his hybrid empirical model. The trilinear shape was deduced from regression analysis of small-to-moderate magnitude earthquakes (Atkinson and Mereu, 1992; Atkinson, 2004). At hypocentral distances (R) < 70 km, direct waves decay relatively steeply (1/R decay in AB95, or $1/R^{1.3}$ decay in AB06). Then there is a "transition zone" of low attenuation (or even increasing amplitudes) as the direct wave is joined by strong post-critical reflections from the Moho (Burger et al.,1987; Somerville et al., 1990; Ou and Herrmann, 1990). At large distances (>150 km), the Lg phase (reflected and refracted shear wave multiples) predominates, and a slower surface-wave spreading applies, with associated anelastic attenuation effects (Kennett, 1986; Ou and Herrmann, 1990).

An interesting feature of the Val-des-Bois attenuation is that the Moho bounce effect appears to be pushed out to relatively large distances, beyond 200 km. It may also extend

over a large distance range, if the elevated amplitudes near 60 km are resulting from the first bounce off the Moho. The nature of the Moho bounce, including the distance range over which it extends, is strongly influenced by focal depth, mechanism and crustal structure (Burger et al., 1987; Ou and Herrmann, 1990; Bowman and Kennett, 1991). The relatively deep focus of the Val-des-Bois event (22 km) may thus be a factor in the large-amplitude PSA values observed from 60 to 300 km. The 1988 **M**5.8 Saguenay, Quebec earthquake was even deeper (28 km), and also showed a predominant Moho bounce effect that was partly attributed to its depth (Somerville et al., 1990; Boore and Atkinson, 1992); the Saguenay earthquake also resulted in a dramatic under-prediction of ground motions by GMPEs in the distance range affected by the Moho bounce. Data from the Val-des-Bois earthquake, used in combination with waveform modeling, may shed new light on Moho bounce effects in ENA, from both this event and the Saguenay earthquake. This will be fertile ground for further detailed studies.

The apparent complexity in the decay of ground-motion amplitudes due to wave propagation effects in ENA tend to support an earlier (and prophetic) assertion of Shin and Herrmann (1987), that the Lg amplitudes at regional distances may be the most robust indicators of source parameters. The Lg phase provides a good sample of the focal sphere and inherently averages effects at receiver stations over a wide range of incident angles; it is relatively free of the complications of wave propagation that are evidenced at closer distances due to the effects noted above. On Figure 2, we observe that the Val-des-Bois ground-motion amplitudes behave in a stable and predictable manner for R>300 km, and are in accord with recent GMPEs (for rock sites) in this distance range. It may be that ground motions at closer distances are inherently difficult to predict with average GMPEs, as the details of the location and strength of the transition zone are event-specific, and only "smear out" to a general pattern when averaged over many events. The Val-des-Bois earthquake joins other recent ENA events, in particular the Riviere du Loup and Saguenay events, in emphasizing the need for better-constrained GMPE models to predict motions at <100 km in ENA. Our current predictive models are obviously doing a poor job in this critical distance range.

Intensity Data

There were over 56,000 responses to the U.S. Geological Survey's DYFI online intensity questionnaire for the Val-des-Bois earthquake, with several thousand more local responses to the same questionnaire on the Geological Survey of Canada site. The maximum reported intensity was VII. The difference between the two sites is that Canadian responses on the USGS site are coded by city location, whereas the responses on the GSC site are coded by postal code. Responses on the GSC site provide more local detail within towns and cities, but are sparse as the site was not immediately available and the GSC data are not available in real time. The two datasets were merged to produce a composite list of reported MMI at various localities; this may have resulted in some "double-counting" of responses, as some people may have responded online to both the USGS and GSC. The MMI data were then binned in distance bins 0.1 log units in width, to characterize the average behavior of intensity versus distance, using the binning procedure described by Atkinson and Wald (2007). The MMI attenuation is shown in Figure 3, along with the intensity GMPE of Atkinson and Wald (2007) for ENA.

Interestingly, the observed intensities in the distance range from 100 to 300 km are generally lower than predicted amplitudes for an event of this size, contrary to the behavior for the instrumental data (which were under-predicted in this distance range). At close distances (<40 km), observed intensities are higher than predicted by AW2007, though data are sparse and scatter widely.

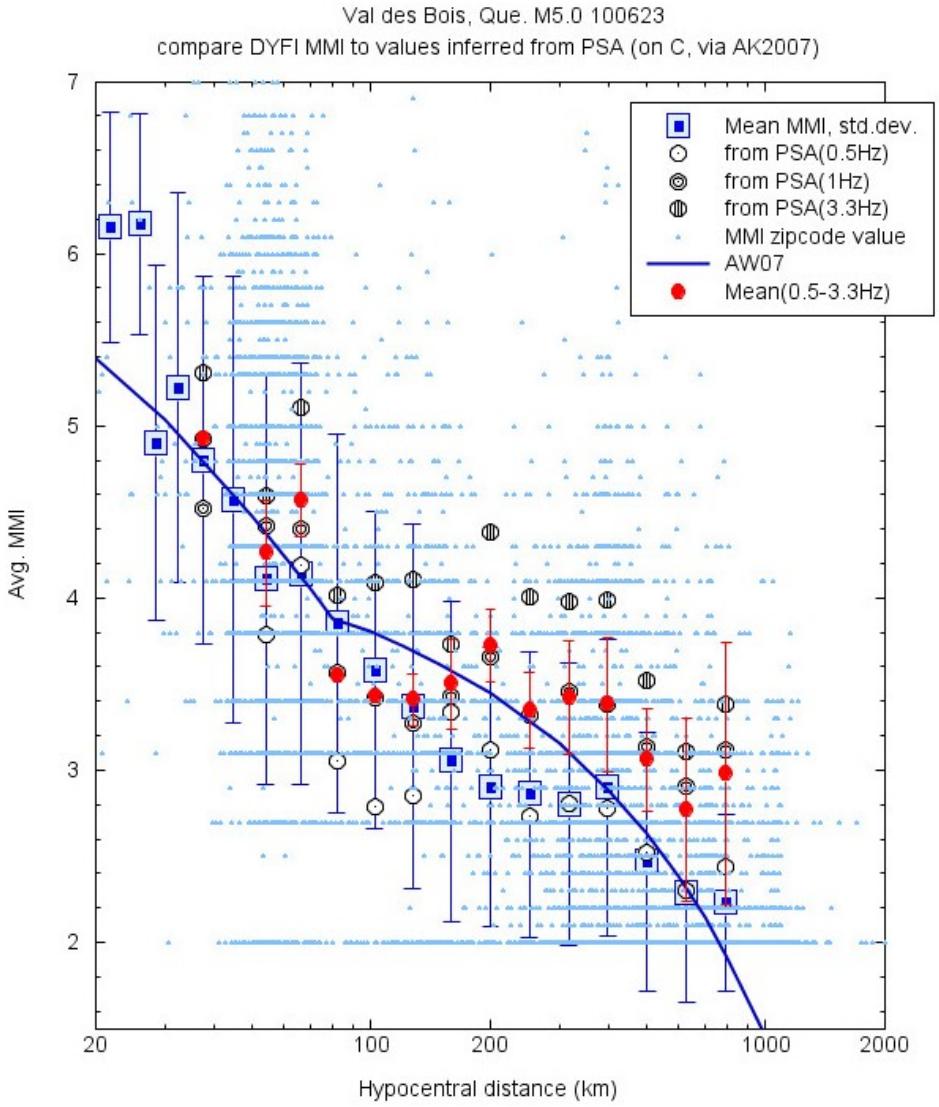

Figure 3 *– Intensity observations from the Val-des-Bois earthquake (as of July 21, 2010). Light grey dots are individual DYFI reports from USGS and GSC. Blue boxes with error bars show binned mean MMI and standard deviation from these reports. Black symbols show mean binned MMI inferred from instrumental data, using the relationships of Atkinson and Kaka (2005). Standard deviations of instrumental MMI shown only for mean measure (0.5, 1, 3.3 Hz (red symbols)). Line is prediction equation of Atkinson and Wald (2007).*

To see if the intensity data can shed light on the instrumental ground-motion observations (and vice versa), we wish to overlay the two types of information. This can be done by

transforming the instrumental data into equivalent intensity values, using empirical relationships between PSA and MMI; the inferred "instrumental intensities" can then be binned and plotted against distance in the same way as the DYFI intensity data. Complications in this process include the potential differences in site conditions between the DYFI and instrumental data, and the fact that the DYFI intensity is a single value at any point, while the instrumental data have a range of amplitudes depending on frequency. The DYFI intensities presumably reflect some frequency range of the ground motion spectrum, for some average site condition. We make the assumption that the DYFI intensity data correspond to an average site condition of C (500 m/s shear-wave velocity), which is a prevalent regional site condition. We correct each instrumental ground motion spectrum to an equivalent spectrum on C, using conversion factors from rock (A) to B/C from Atkinson and Boore (2006), and from B/C to other site conditions from Boore and Atkinson (2008). This is a very crude correction that may not adequately account for actual site amplifications (which may be large, as discussed earlier). However, it may also be noted that the DYFI intensity data, when binned against distance, implicitly average observed effects over a wide range of site conditions, and may thus also tend to filter out extreme site effects. We use the relationships of Atkinson and Kaka (2007), for the given magnitude and distance of each ground-motion observation (after correction to site class C), to predict MMI from PSA at 0.5 Hz, 1 Hz and 3.3 Hz. Thus we have three estimates of intensity for each instrumental ground motion observation, each of which comes from a different part of the ground motion spectrum. We bin these intensity estimates in the same way as the DYFI data, and plot them on Figure 3, along with the mean instrumental MMI predicted from all three of the PSA-based MMI measures (PSA at 0.5Hz, 1 Hz, 3.3 Hz)The standard deviation of the instrumental intensity is shown only for the mean measure (for bins with 3 or more observations), to avoid further cluttering the plot. It may be noted that MMI estimated from PGA is very close to that estimated from PSA at 3.3 Hz, while MMI estimated from PGV is very close to that estimated from PSA at 1 Hz. We did not include the MMI estimates from PGA and PGV on Figure 3, also to avoid clutter.

The intensity estimates from 0.5 Hz PSA track the observed values well at distances >150 km. At closer distances, the average of the three inferred MMI values (PSA from 0.5, 1, 3.3 Hz) is in reasonable accord with the observations. The MMI that would be inferred from the high frequency ground motions (either 3.3 Hz PSA or PGA) is significantly higher than observed values at larger distances (>100 km). The large observed amplitudes for high-frequency instrumental ground motions at distances of 200 to 300 km, would suggest that elevated felt effects might have been reported in this distance range, but they were not.

Attenuation and Source Characteristics

We use the Fourier spectra for records on rock sites (A or B) within 1000 km to examine the attenuation and source characteristics of the Val-des-Bois earthquake. Figure 4 plots the attenuation of Fourier acceleration on rock sites at two frequencies, in comparison to the predicted FA attenuation according to the empirical attenuation model of Atkinson (2004). The data and corresponding prediction equation for the 2005 **M**4.7 Riviere du Loup earthquake are also shown for comparison. The A04 curves are plotted for m1=4.9,

which is the predicted m1 value for **M**=5.0 (from Atkinson, 2004), and m1=4.7, which is the predicted value for **M**=4.7. (Note: m1 is the 1-Hz magnitude measure of Chen and Atkinson (2002), which was used by A04 as the predictive variable for the overall level of the attenuation curves; A04 also provided an empirical relationship between m1 and **M**.) Both horizontal components are plotted, plus the vertical component converted to horizontal by multiplying by a frequency-dependent factor for rock sites in eastern Canada from Siddiqqi and Atkinson (2002). The H/V factor is near unity at 1 Hz, increasing to a maximum value of 1.6 at 10 Hz. It is noteworthy that in the AB06 GMPEs, the Atkinson (2004) attenuation shape was used for the attenuation model, and the Siddiqqi and Atkinson (2002) H/V ratio was used as an estimate of site response for hard rock sites.

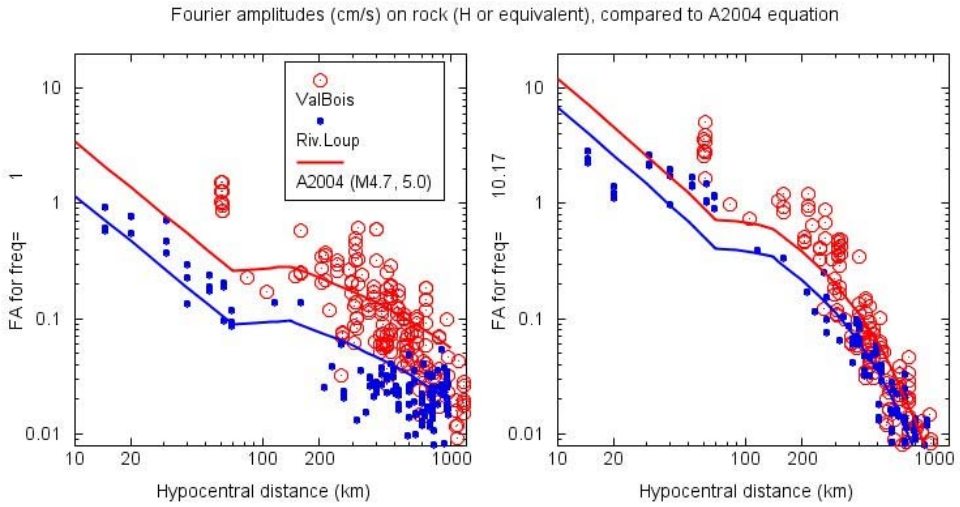

Figure 4 *– Fourier acceleration on rock sites (A/B) for the Val-des-Bois and Riviere du Loup earthquakes, compared to attenuation model of Atkinson (2004), for 1 and 10 Hz (in cm/s).*

Inspection of Figure 4 reveals the same general features that were noted in the PSA data, although the under-prediction of near-source amplitudes appears less pronounced. The ground-motion data are well-behaved at large distances, but the average A04 attenuation shape does not do a good job of projecting distant amplitudes back to the source. It was demonstrated through plots of residuals in Atkinson (2004) that the attenuation shape accurately describes the average attenuation of FA for the database studied, which included 1700 records from events of M 3 to 5, at distances from 10 to 1000 km. Moreover, earlier significance tests verified that the trilinear form is a significantly better fit to the FA data on average than either a linear or bilinear form (Atkinson and Mereu, 1992). Thus we do not think that the fitting problem lies in the trilinear attenuation shape being "wrong", at least as an ensemble average. Rather, we hypothesize that there may be a basic problem in applying an average ensemble shape to individual events, because the details of the shape, and in particular how the transition zone works to tie the near-source motions to regional observations, may vary significantly from event to event – and might possibly be different for large versus small events. Observations are most

numerous at regional distances and will thus dictate the "level" of the curve, leading to a "tail wagging the dog" problem that confounds the prediction of near-source amplitudes (see also Boore et al., 2010). We suggest that the solution lies in changing the way the distant data are used to infer source characteristics. In a nutshell, the distant observations should be heavily weighted in determining the relative average strength of the motion at different frequencies, due to their stability. This relative strength of the source (ie. source spectral shape) can be determined by removing anelastic attenuation effects; in other words, we make a shape correction to the spectrum based on the model for Q, the regional Quality factor. The seismic moment of the event can be used to constrain the near-source level of the spectrum, effectively tying the determined spectral shape back to a fixed source reference level. This places emphasis on the aspects of the source and attenuation that are most robustly determined: the seismic moment, and the Q model.

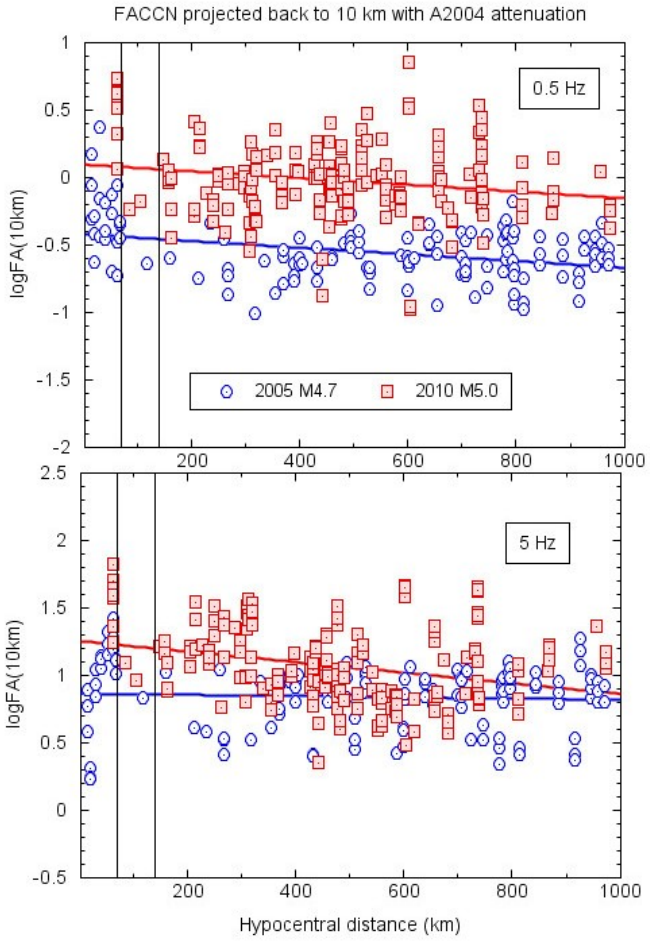

Figure 5 *– Estimates of logFA at 10 km (rock sites) obtained by "playing back" the Atkinson (2004) attenuation model, for the Val-des-Bois and Riviere du Loup events, at 0.5 and 5 Hz. Vertical lines indicate the transition zone boundaries of 70 km and 140 km for reference. The intercept of logFA(10km) versus R represents a Q-corrected estimate of the spectral level.*

The approach is illustrated in Figure 5, in which we plot the $\log_{10}$ FA values, corrected back to a reference distance of 10 km using the Atkinson (2004) attenuation model. The amplitudes are plotted against distance on a linear scale, to emphasize the distant observations. On a linear scale, the fact that the overall level is controlled largely by distant observations is apparent, and the near-source amplitude trends appear less important. If the A04 attenuation model were a perfect fit to the shape of the amplitude decay, then the best-fit line of logFA(10km) versus R would be a straight line with a slope of zero. For these two events, the fitted line has a slightly negative slope, consistent with our observation that the near-source observations are under-predicted. The persistence of the negative slope with distance implies that the anelastic attenuation is somewhat larger than that in the A04 model. The y-intercept of the line provides our initial estimate of the spectral amplitude at 10 km for a specific frequency. The y-intercept is essentially a Q-corrected spectral amplitude, with a constant for geometric spreading added. Note that we could obtain the same estimate of the 10-km spectral amplitude at each frequency by "fine-tuning" the Q model to match the slope of log A versus R for each event and frequency; the use of the y-intercept is equivalent to an event-specific Q correction. A key point is that it is the geometric spreading constant, and thus the absolute level of the spectrum, that is highly uncertain. By contrast, Q is robustly determined on average by distant observations, and can be fine-tuned to closely match individual events (as in Figure 5). Specifically, Q studies conducted in ENA over the last 25 years have tended to produce very similar results (eg. Hasegawa, 1985; Shin and Herrmann, 1987; Woodgold, 1990; Atkinson and Mereu, 1992; Boatwright,2004; Benz et al., 1997; Atkinson, 2004). Because Q is well constrained, the relative level of the spectrum between frequencies (ie. the shape) can be determined with reasonable confidence. We have determined it here by taking the intercept of attenuation-corrected amplitudes at all distances. Alternatively, we could have corrected just the Lg observations (beyond 140 km) for attenuation to any reference distance and averaged them; this would produce an equivalent source spectral shape because the distant observations dominate the fit.

Having determined the spectral shape at the source, it remains to scale it up from 10 km to the source (1 km), using the seismic moment as a constraint on the absolute level of the spectrum. Figure 6 plots the attenuation-corrected apparent source spectrum (R=1km), scaled up by adding a constant (in log units), such that the long-period end of the spectrum matches the level for a Brune source spectrum for the given seismic moment (see Brune, 1970; Boore, 1983). The stress drop of the Brune model is chosen to approximately match the high-frequency spectral level (see Boore, 1983). All factors and constants for setting the level of the Brune source spectrum, including crustal amplification, radiation pattern and physical constants, are as implemented in Atkinson and Boore (2006); note that the absolute level of the spectrum as set by these factors is not particularly important, as we are scaling to match the moment end of the spectrum. The source spectrum obtained for the 2010 Val-des-Bois (**M**5.0) earthquake is matched by a Brune spectrum with a stress drop of 250 bars; the 2005 Riviere du Loup (**M**4.7) spectrum is matched by a Brune spectrum with a stress drop of 150 bars. These are approximate values, as no formal fitting was done. We used the same process to produce apparent source spectra for three other relatively-well recorded ENA events that have

known moment magnitudes (from moment tensor solutions) of **M**4.5 to 5.0 (data from Assatourians and Atkinson, 2008, with moment magnitudes from Atkinson and Boore, 2006 and Boore et al., 2010); these spectra are also plotted on Figure 6 for comparison. The 2002 **M**5.0 Au Sable Forks event had a stress drop near 150 bars, and shows a significant spectral sag; this agrees with other reported source spectra for this event, as obtained by empirical Greens function techniques, from Atkinson and Sonley (2003) and Viegas et al. (2010). The 1997 **M**4.5 event has a stress drop near 300 bars, while the 1999 event has a stress drop near 150 bars. Thus the Val-des-Bois event appears to have had a relatively high stress drop – though not as high as the value of 500 bars attributed to the 1988 Saguenay event (Boore and Atkinson, 1992).

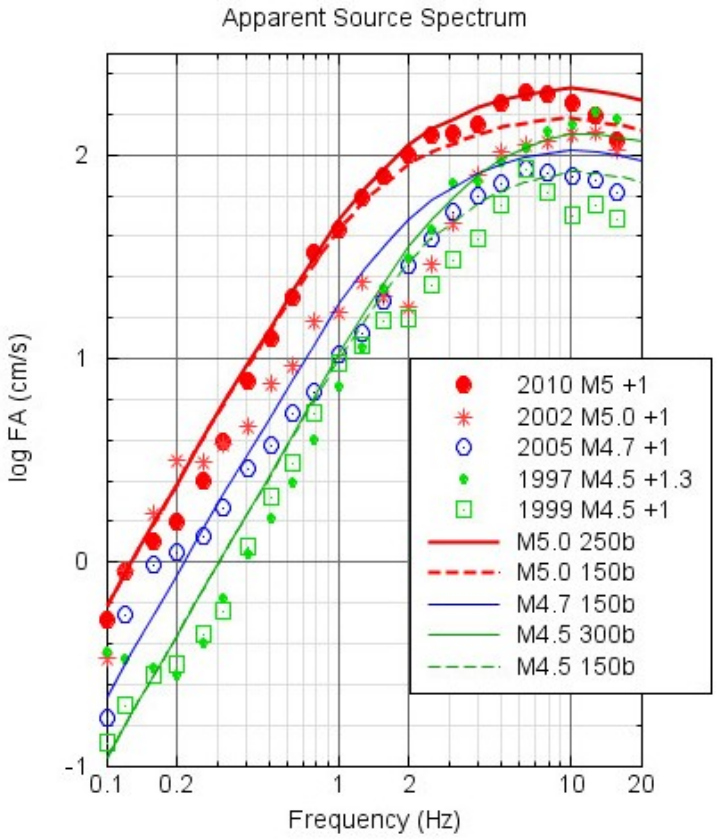

Figure 6 *– Source spectrum of 2010 Val-des-Bois, 2005 Riviere du Loup, and other* ***M****4.5-5.0 events with known moment.*

Interestingly, the constant added for all 5 events, in order to bring the log FA(10km) spectra up to the level fixed by the seismic moment, is approximately +1.0 log units (+1.0 for all events except the 1997 event, for which it is +1.3). In the context of the A04 attenuation model, this would imply that the correct source level is obtained if one assumes the A04 geometric spreading model for hypocentral distances beyond 10 km ($R^{-1.3}$ from 10 to 70 km, $R^{+0.2}$ from 70 to 140 km, then $R^{-0.5}$ beyond 140 km), but applies 1/R to go from 10 km to 1 km (ie. use 1/R from the hypocenter up to the epicenter, for a typical focal depth of 10 km, then attenuate as $R^{-1.3}$ from the epicenter to 70 km). This is

admittedly a crude way of looking at the attenuation, which as we have seen is complex and often defies such simplistic descriptions. Nevertheless, it is interesting that the required scaling factor appears to be relatively stable. This suggests that it may be possible to develop a better attenuation model, possibly involving more event parameters, which would more accurately describe the attenuation of ENA amplitudes over a broad distance range. The development of such an improved model should be undertaken with a combination of modeling and analysis of empirical data.

Summary and Implications for GMPEs

The 2010 Val-des-Bois, Quebec earthquake produced a rich instrumental and felt ground motion database. We have presented instrument-corrected response spectra and Fourier data from 120 stations, at distances from 60 to 1000 km, and compared them to recent ground motion models. We have also compared the ground-motion data to the intensity data collected from online DYFI surveys. The Val-des-Bois earthquake produced relatively-large response spectral amplitudes at distances less than 200 km, greater than predicted by most recent GMPEs (including the Atkinson and Boore, 2006 equations). By contrast, reported intensities at regional distances tended to be smaller than predicted by intensity GMPEs (Atkinson and Wald, 2007). From recent earthquakes (Val-des-Bois and the 2005 Riviere du Loup event), we have learned that amplitudes at near distances are not well predicted by average attenuation shapes drawn to pass through regional observations. To infer the source spectrum or near-source motions, we suggest the use of seismic moment as a constraint on the level of the source spectrum. Using Q-corrected observations to deduce the source-spectral shape, and the known seismic moment to fix its absolute amplitude level, we obtain an apparent source spectrum for the Val-des-Bois earthquake that is well described by a Brune model with a stress drop of 250 bars.

Data from the 2010 Val-des-Bois and 2005 Riviere du Loup earthquakes suggest that the GMPEs of Atkinson and Boore (2006) tend to under-predict response spectral amplitudes from moderate events (**M**~5), most particularly in the distance range from 30 to 60 km. Recent studies have compared response spectra from small-to-moderate events in ENA to those in California (Atkinson and Morrison, 2009; Atkinson et al., 2010). At distances <60 km, PSA values for frequencies of 1 to 3.3 Hz are essentially the same within the two regions, for a reference site condition (B/C boundary). Regression of small-magnitude data (from both regions) suggests that the AB06 equations are under-predictions for **M**5 in ENA, while the Boore and Atkinson (2008) NGA equations are over-predictions for **M**5 in California. The AB06 predictions for **M**5 in ENA lie below the BA08 predictions for **M**5 in California, for B/C sites, except at high frequencies (see Atkinson and Boore, 2006 and Atkinson and Morrison, 2009). At larger magnitudes (**M** 6 to 7), the AB06 and BA08 equations are in closer agreement; the AB06 equations may tend to over-predict near-source amplitudes because they do not contain the saturation effects incorporated into the BA08 model. Given the agreement between AB06-ENA and BA08-California at larger magnitudes, and the agreement of moderate-magnitude data in the two regions, we speculate that the AB06 equations are probably reasonable for events of **M**≥6 in ENA, while acknowledging an apparent under-prediction of AB06 for **M**~5. Future work will focus on resolving near-source attenuation issues to provide better GMPEs for ENA over all magnitudes.

Data and Resources

Seismographic data for Canada were obtained from the Earthquakes Canada AutoDRM facility at http://earthquakescanada.nrcan.gc.ca/stndon/AutoDRM/autodrm_req-eng.php

(accessed June 24, 2010); U.S. seismograph data were obtained from the IRIS AutoDRM facility at http://www.iris.edu/SeismiQuery/breq_fast.phtml

(accessed July 9, 2010). Unprocessed strong-motion data were obtained from the Geological Survey of Canada, at http://earthquakescanada.nrcan.gc.ca/index-eng.php (accessed June 25, 2010)(Lin and Adams, 2010). Processing was performed using the Engineering Seismology Toolbox software of Assatourians and Atkinson (2008) (www.seismotoolbox.ca). Our processed time series and tables of PSA and FA for the event may be downloaded from www.seismotoolbox.ca. Earthquake magnitude, focal mechanism and depth were provided by Bob Herrmann on his web site at http://www.eas.slu.edu/Earthquake_Center/MECH.NA/20100623174142 (accessed June 25, 2010). Intensity data were downloaded from the U.S. Geological Survey DYFI site at http://earthquake.usgs.gov/earthquakes/dyfi/ (accessed June 28, 2010), and obtained from the Geological Survey of Canada for the local area (S. Halchuk, pers. comm. June 28, 2010). All figures were made using COPLOT (www.cohort.com).

Acknowledgements

These analyses were made possible through the excellent autodrm services provided by the Geological Survey of Canada and IRIS. We are grateful to John Adams and Lan Lin of the GSC for quickly providing the strong-motion data, and to Stephen Halchuk for providing the GSC intensity reports. We thank Alireza Babaie Mahani for assistance with processing of the U.S. seismographic data. We thank Martin Chapman and Dave Boore for constructive review comments; we are also indebted to Martin Chapman for pointing us towards some IRIS stations that we had initially missed. The Engineering Seismology Toolbox project that made the rapid analysis and dissemination of these data possible is funded by the Canadian Foundation for Innovation and the Natural Sciences and Engineering Research Council of Canada.

References

Atkinson, G. (2004). Empirical attenuation of ground motion spectral amplitudes in southeastern Canada and the northeastern United States. Bull. Seism. Soc. Am.,**94**, 1079-1095.

Atkinson, G. (2008). Alternative ground-motion prediction equations for eastern North America from a Referenced Empirical Approach: Implications for epistemic uncertainty. Bull. Seism. Soc. Am., **98**, 1304-1318

Atkinson , G., K. Assatourians and E.A. Nicol (2010). Comparisons of ground-motion attenuation in eastern North America versus California. Seism. Res. L., **81**, 291.

Atkinson, G., and D. Boore (1995). New ground motion relations for eastern North America. Bull. Seism. Soc. Am., **85**, 17-30.

Atkinson, G. and D. Boore (2006). Ground motion prediction equations for earthquakes in eastern North America. Bull. Seism. Soc. Am., **96**, 2181-2205.

Atkinson, G. and S. Kaka (2007). Relationships between felt intensity and instrumental ground motions for earthquakes in the central United States and California. Bull. Seism. Soc. Am., **97**, 497-510.

Atkinson, G. and R. Mereu (1992). The shape of ground motion attenuation curves in southeastern Canada. Bull. Seism. Soc. Am., **82**, 2014-2031.

Atkinson, G. and M. Morrison (2009). Regional variability in ground motion amplitudes along the west coast of North America. Bull. Seism. Soc. Am., **99**, 2393-2409.

Atkinson, G. and E. Sonley (2003). Ground motions from the 20 April, 2002 Au Sable Forks, NY earthquake. Seism. Res. L., **74**, 330-349.

Atkinson, G. and D. Wald (2007). Modified Mercalli Intensity: A surprisingly good measure of ground motion. Seism. Res. L., **78,** 362-368.

Assatourians, K. and G. M. Atkinson (2008). Program: ICORRECT, Report, University of Western Ontario , London, ON, Canada (CAN), Canada (CAN). http://www.seismotoolbox.ca/ICORRECT/ICORRECT.pdf

Assatourians, K., and G. Atkinson (2010). Database of processed time series and response spectra for Canada: An example application to study of the 2005 MN5.4 Riviere du Loup, Quebec earthquake. Seism. Res. L., submitted.

Benz, H., A. Frankel and D. Boore (1997). Regional Lg attenuation for the continental United States using broadband data. Bull. Seism. Soc. Am., **87**, 606-619.

Boatwright, J. (1994). Regional propagation characteristics and source parameters of earthquakes in eastern North America. Bull. Seism. Soc. Am., **84**, 1-15.

Boore, D. (1983). Stochastic simulation of high-frequency ground motions based on seismological models of the radiated spectra. Bull. Seism. Soc. Am., **73**, 1865-1894.

Boore, D. and G. Atkinson (1992). Source spectra for the 1988 Saguenay, Quebec earthquakes. Bull. Seism. Soc. Am., **82**, 683-719.

Boore, D. and G. Atkinson (2008). Ground-motion prediction equations for the average horizontal component of PGA, PGV, and 5%-damped SA at spectral periods between 0.01s and 10.0 s. Earthquake Spectra, **24**, 99-138.

Boore, D., K. Campbell and G. Atkinson (2010). Determination of stress parameters for eight well-recorded earthquakes in eastern North America. Bull. Seism. Soc. Am., **100**, in press.

Bowman, J. and B. Kennett (1991). Propagation of Lg waves in the North Australian craton: Influence of crustal velocity gradients. Bull. Seism. Soc. Am., 81, 592-610.

Brune, J. (1970). Tectonic stress and the spectra of seismic shear waves from earthquakes. J. Geophys. Res., **75**, 4997-5009.

Burger, R., P. Somerville, J. Barker, R. Herrmann, and D. Helmberger (1987). The effect of crustal structure on strong ground motion attenuation relations in eastern North America. Bull. Seism. Soc. Am., **77**, 420-439.

Campbell, K. (2003). Prediction of strong-ground motion using the hybrid-empirical method and its use in the development of ground-motion (attenuation) relations in eastern North America. Bull. Seism. Soc. Am., **93,** 1012-1033.

Chen, S. and G. Atkinson (2002). Global comparisons of earthquake source spectra. Bull. Seism. Soc. Am., **92**, 885-895.

Hasegawa, H. (1985). Attenuation of Lg waves in the Canadian shield. Bull. Seism. Soc. Am., 75, 1569-1582.

Kennett, B. (1986). Lg waves and structural boundaries. Bull. Seism. Soc. Am., **76**,1133-1141.

Lin, L. and J. Adams (2010). Strong Motion Records of the Val-des-Bois, Québec, Earthquake of June 23, 2010. Canadian Hazard Information Service Internal Report 2010-1.1, 20 pages plus digital appendix.

Motazedian D., J.A. Hunter (2008) "Development of a NEHRP Map for the Orleans Suburb of Ottawa, Ontario", *Canadian Geotechnical Engineering Journal* 45:1180-1188 .

Ou, G. and R. Herrmann (1990). A statistical model for peak ground motion from local to regional distances. Bull. Seism. Soc. Am., **80**, 1397-1417.

Shin, T. and R. Herrmann (1987). Lg attenuation and source studies using 1982 Miramichi data. Bull Seism. Soc. Am., 77, 384-397.

Siddiqqi, J. and G. Atkinson (2002). Ground motion amplification at rock sites across Canada, as determined from the horizontal-to-vertical component ratio. Bull. Seism. Soc. Am., **92**, 877-884.

Somerville, P., J. McLaren, C. Saikia and D. Helmberger (1990). The Nov. 25, 1988 Saguenay, Quebec earthquake: source parameters and the attenuation of strong ground motion. Bull. Seism. Soc. Am., **80**, 1118-1143.

Viegas, G., R. Abercrombie and W. Kim (2010). The 2002 M5 Au Sable fork, NY, earthquake sequence: source scaling relationships and energy budget. J. Geophys. Res., in press.

Wald, D., V. Quitoriano, T. Heaton, H. Kanamori, C. Scrivner and C. Worden (1999). TriNet ShakeMaps: Rapid generation of peak ground motion and intensity maps for earthquakes in southern California. Earthquake Spectra, **15**, 537-555.

Woodgold, C. (1990). Estimation of Q in eastern Canada using coda waves. Bull. Seism. Soc. Am., **80**, 411-429.

Table 1 – Stations recording the Val-des-Bois earthquake. For more details, see www.seismotoolbox.ca

Station	Latitude	Longitude	Epicentral Distance	Soil condition	Site Class	V_{S30}	Comment
OTT	45.394	-75.717	58.7	Bedrock	A	1835	good
OTGH	45.401	-75.697	57.5	Thin soil	A	1926	peak 20to30hz(all3comp)
OTNM	45.412	-75.689	56.2	Soil	E	150	strong resonance peaks at 2, 4 Hz (factor of 10)
OTRS	45.460	75.496	48.9	Soil	E	144	strong response peak at 1Hz, factor of 10
OT002	45.474	-75.502	47.3	Clay	D	188	strong response at f<2Hz
OT004	45.364	75.775	63.3	Clay or till	B	898	Lpnoise(or response) at f<0.6hz
OT006	45.429	-75.650	53.6	till	B	900	Lpnoise(or response) at f<0.8hz
OT008	45.350	-75.642	62.2	Sand	C	580	strong peak at 2Hz
OT012	45.394	75.717	58.7	Bedrock	A	1835	Lpnoise at f<0.6hz
MO001	45.510	-73.553	157.2	unknown	D	200	Lpnoise f<2Hz, small peak f~5hz?(<factor2)
MO002	45.496	-73.553	157.7	unknown	D	200	Lpnoisef<2hz, small peak f 4to5hz?
MO003	45.543	-73.571	154.9	unknown	D	200	Lpnoisef<5hz, flat response
MO004	45.513	-73.584	154.9	unknown	D	200	Lpnoisef<5hz, flat response
OTT	45.394	-75.717	60.1	rock	A	1914	Clipped
PEMO	45.677	-77.247	138.8	soil	C	591	large apparent H/V f>3hz
PLVO	45.040	-77.075	157.2	rock	A	2000	excellent
ALGO	45.954	-78.051	198.3	soil	D	354	large apparent H/V f2to10hz
KGNO	44.227	-76.493	203.3	rock	A	2000	very good
BANO	45.020	-77.928	214.6	Thin soil	B	1000	apparent site response at f>=10hz
ALFO	45.628	-74.884	56.6	till	B	1000	
BELQ	47.398	-78.687	295.1	rock	A	2000	
BUKO	45.442	-79.399	307.8	till	B	1000	
CRLO	46.038	-77.380	146.4	rock	A	2000	
DPQ	46.680	-72.777	226.3	rock	A	2000	
EEO	46.641	-79.073	287.1	rock	A	2000	
GAC	45.703	-75.478	22.4	rock	A	2000	Clipped
GRQ	46.607	-75.860	83.1	rock	A	1889	
LATQ	47.384	-72.782	264.9	rock	A	2000	
MOQ	45.312	-72.254	261.0	rock	A	2000	
PECO	43.934	-76.994	249.0	rock	B	1000	
SADO	44.769	-79.142	311.9	rock	A	2000	
TRQ	46.218	-74.551	81.0	rock	A	2000	
VLDQ	48.190	-77.757	306.8	rock	A	2000	
WBO	45.000	-75.275	102.1	till	A	1734	
WLVO	43.924	-78.397	317.6	till	B	1137	
A11	47.243	-70.198	431.9	rock	A	2000	
A16	47.471	-70.006	454.0	rock	A	2000	
A54	47.457	-70.413	424.9	rock	A	2000	
A61	47.693	-70.090	457.5	rock	A	2000	
ACTO	43.609	-80.062	442.1	till	B	966	
BMRO	44.595	-81.217	471.3	soil	C	500	
CHGQ	49.911	-74.375	453.8	rock	A	2000	
CLWO	44.449	-80.301	410.2	soil	C	500	
DAQ	47.964	-71.243	396.4	rock	A	2000	
DREO	43.872	-78.704	339.2	soil	C	500	
DRWO	43.872	-78.730	340.8	soil	C	500	
KILO	48.497	-79.723	430.6	rock	A	2000	
KLBO	45.357	-80.213	372.1	rock	A	2000	
LMQ	47.549	-70.326	434.9	rock	A	2000	
MEDO	43.165	-78.455	384.7	soil	C	500	
PKRO	43.964	-79.071	354.9	soil	C	403	

QCQ	46.779	-71.276	338.6	rock	A	2000	
STCO	43.210	-79.171	418.1	soil	C	415	
SUNO	46.644	-81.344	457.3	rock	A	2000	
TORO	43.614	-79.343	396.7	soil	D	303	
TYNO	43.095	-79.870	467.1	soil	C	404	
A64	47.826	-69.892	477.1	rock	A	2000	
BASO	44.013	-81.665	529.3	soil	C	500	
BATG	47.277	-66.060	737.4	rock	A	2000	
BRCO	44.244	-81.442	502.4	soil	D	282	
BWLO	44.117	-81.138	486.3	soil	C	500	
CNQ	49.302	-68.074	672.9	rock	A	2000	
ELFO	43.193	-81.316	551.3	soil	C	451	
GGN	45.117	-66.822	682.0	rock	A	2000	
GSQ	48.914	-67.111	714.6	rock	A	2000	
HAL	44.638	-63.592	942.3	rock	A	2000	
ICQ	49.522	-67.272	735.4	rock	A	2000	
KAPO	49.450	-82.508	656.8	rock	A	2000	
LG4Q	53.627	-74.097	865.5	rock	A	2000	
MALO	50.024	-79.764	557.9	rock	A	2000	
MNQ	50.533	-68.774	716.5	rock	A	2000	
PLIO	41.751	-82.628	735.6	rock	A	2000	
PNPO	48.596	-86.285	867.6	rock	A	2000	
SMQ	50.223	-66.703	811.0	rock	A	2000	
TIMO	48.466	-81.303	523.5	rock	A	2000	
TOBO	45.226	-81.523	475.6	rock	A	1000	
YOSQ	52.867	-72.200	810.8	rock	A	2000	
GBN	45.408	-61.513	1088.1	rock	A	2000	
GTO	49.746	-86.961	956.2	rock	A	2000	
NATG	50.287	-62.810	1060.1	rock	A	2000	
SCHQ	54.832	-66.833	1166.9	rock	A	2000	
SILO	54.479	-84.913	1164.7	rock	A	2000	
TBO	48.647	-89.409	1092.4	rock	A	2000	
VIMO	52.817	-83.745	973.3	rock	A	2000	
ACCN	43.380	-73.670	316.0	rock	A	2000	
ALLY	41.650	-80.140	602.7	rock	A	2000	
BRNJ	40.680	-74.570	586.4	rock	A	2000	
BRNY	41.410	-74.010	514.4	rock	A	2000	
CPNY	40.790	-73.960	582.7	rock	A	2000	
FOR	40.860	-73.890	576.3	rock	A	2000	
HCNY	42.700	-74.400	367.2	rock	A	2000	
LUPA	40.600	-75.370	590.5	rock	A	2000	
MMNY	42.730	-77.910	402.2	rock	A	2000	use 100s/s records only
MSNJ	40.880	-74.180	569.3	rock	A	2000	
MVL	40.000	-76.350	660.9	rock	A	2000	
NPNY	41.750	-74.140	475.1	rock	A	2000	
ODNJ	41.080	-74.610	541.8	rock	A	2000	
PAL	41.010	-73.910	559.7	rock	A	2000	
PANJ	40.380	-74.700	618.3	rock	A	2000	
PRNY	42.470	-76.540	391.2	rock	A	2000	
PTN	44.570	-74.980	154.0	soil	C	500	amplitudes suspect at f>1Hz
SDMD	39.410	-76.840	731.2	rock	A	2000	
UCCT	41.790	-72.230	527.6	soil	C	500	5Hz site response peak(factor3?)
WCNY	43.980	-75.650	214.5	rock	A	2000	
FFD	43.470	-71.654	407.3	soil	C	500	~3Hz site response peak
HNH	43.705	-72.287	352.4	rock	A	2000	
QUA2	42.279	-72.352	475.6	rock	A	2000	

WES	42.385	-71.322	514.5	rock	A	2000	
WVL	44.565	-69.662	480.7	rock	A	2000	
YLE	41.317	-72.921	551.6	rock or thin soil	A	2000	may be amplification at f>8Hz
PSWB	41.306	-76.015	514.3	Soil	C	500	~3Hz spectral peak
UPAO	40.482	-80.022	707.1	soil	C	500	~3Hz spectral peak
WRPS	40.794	-77.865	601.0	rock	A	2000	
PLIO	41.751	-82.628	736.4	rock	A	2000	
AAM	42.301	-83.657	765.9	Soil	C	500	0.5Hz-2Hz spectral peak
CBN	38.205	-77.373	871.7	soil	C	500	high amplitudes and H/V at low frequencies
GLMI	44.825	-84.617	723.6	soil	C	500	incorrect instrument reponse, delete
LONY	44.620	-74.583	160.3	rock	A	1000	high-freq shape may be amplified?
NCB	43.971	-74.224	237.8	rock	A	2000	
PKME	45.264	-69.292	488.1	rock	A	2000	
CUNY	45.910	-75.490	591.9	soil	C	500	